SYNTHESIS OF α-Al$_2$O$_3$ BASED FOAMS WITH IMPROVED PROPERTIES AS CATALYST CARRIERS

SINTETIZIRANE PENE NA OSNOVI α-Al$_2$O$_3$ Z IZBOLJŠANIMI LASTNOSTMI KOT NOSILKE KATALIZATORJA

Vesna Nikolić[1], Željko Kamberović[2], Zoran Anđić[3], Marija Korać[2], Miroslav Sokić[4]

[1]Innovation Center of the Faculty of Technology and Metallurgy, University of Belgrade, Karnegijeva 4, Belgrade, Serbia
[2]Faculty of Technology and Metallurgy, University of Belgrade, Karnegijeva 4, Belgrade, Serbia
[3]Innovation Center of the Faculty of Chemistry, University of Belgrade, Studentski trg 12–16, Belgrade, Serbia
[4]Institute for Technology of Nuclear and other Raw Materials, Franše d'Eperea 86, Belgrade, Serbia
vnikolic@tmf.bg.ac.rs

This paper explores the possibility of synthesising catalyst supports with improved properties. Alumina foams were produced with the polymer replication technique. Representative high- and low-temperature sintering ceramics were selected. Suitable suspension amounts, the clay addition and sintering temperature were determined. A lower sintering temperature was used for an economic enhancement of the process. The sintering was conducted at the temperatures from 1573 K to 1773 K for 60 min. A comparative analysis of the studied systems shows that the best compressive strength of 6.2 MPa was achieved with the system based on the α-Al$_2$O$_3$–25 clay (mass fractions, w/%), polyester foam with 10 PPI, sintered at 1673 K.

Keywords: alumina, reticulated foam, sintering, mechanical properties, catalyst carrier

Članek obravnava možnosti sinteze podlage z izboljšanimi lastnosti za katalizatorje. Izbrane so bile značilne keramike, ki se sintrajo pri visokih ali nizkih temperaturah. Določene so bile primerne vsebnosti suspenzije, dodatki gline in temperature sintranja. Za boljšo ekonomičnost postopka je bila izbrana nižja temperatura sintranja. Sintranje je bilo izvršeno pri temperaturah od 1573 K do 1773 K v trajanju 60 min. Primerjalne analize preučevanih sistemov kažejo, da je bila najboljša tlačna trdnost 6,2 MPa dosežena pri sistemu, ki temelji na α-Al$_2$O$_3$–25 gline (masni deleži, w/%), poliestrski peni z 10 PPI, sintrani pri 1673 K.

Ključne besede: glinica, mrežasta pena, sintranje, mehanske lastnosti, nosilec katalizatorja

1 INTRODUCTION

Reticulated ceramic foams are being intensely researched as catalyst carriers.[1–3] They are mostly produced with the polymer replication method, involving soaking a polymer foam into a ceramic-water suspension, drying and sintering it at the temperatures up to 1973 K.[4,5] In comparison with alumina[4] and alumina-mullite foams,[6,7] which are sintered from 1673 K to 1873 K, significantly lower temperatures are needed for the sintering of cordierite – 1573 K,[8] cordierite-mullite-alumina – 1523 K for 2 h,[9] aluminosilicate – 1523 K for 5 h [10] and porcelain – 1423 K for 5 h,[6] 1523 K for 2 h.[11] It was reported that a polyester foam is more appropriate than polyurethane due to the toxicity of the latter during combustion.[6] The production of porcelain foams involves the drying of green bodies at room temperature for 72 h and then at 373 K for 1 h,[11] instead of 24 h at room temperature.[4,6] Compressive strengths of alumina foams range from 0.27 MPa to 3 MPa.[4,12] Cordierite foams have higher compressive strengths (up to 2 MPa)[8] than alumina mullite (1.11 MPa),[7] alumina (0.59 MPa)[13] and cordierite-mullite-alumina (0.55 MPa).[9] Compressive and flexural strengths of porcelain foams can reach 23.07 MPa and 11.10 MPa, respectively.[11] Aluminosilicate[10] and fine cordierite foams (< 1 mm cell size)[1,14] achieve the pore volumes of about 90 %[10] and 80 % to 85 %,[1,14]

more than porcelain, from 77.4 % to 88.4 % for 60 PPI and 10 PPI (pores per inch) and from 26.28 % to 70.59 %.[6,11] Alumina foams have the pore volumes of 89.5 % and 86.75 % for 12 PPI[13] and between 82 % and 94 % for 5 PPI and 10 PPI,[4] more than alumina-mullite (from 83.4 % to 87.8 % for 10 PPI to 60 PPI)[7] and porcelain.[6,11]

The aim of the current study was an optimisation of the alumina-foam preparation using the polymer replication method. The production cost can be reduced by sintering the foam at a lower temperature. The preliminary results regarding the effects of adding clay were presented in the previous work of the authors.[15] In the present investigation, the polyester foam was soaked into the α-Al$_2$O$_3$ and α-Al$_2$O$_3$ clay-water suspensions. The optimum sintering temperature was determined. Sintered foams with suitable properties were proposed for an additional investigation as primary catalyst carriers.

2 EXPERIMENTAL SECTION

Initial investigations included a microstructural analysis of the starting powders, the α-Al$_2$O$_3$ and α-Al$_2$O$_3$ clay mixtures. The microstructure was analysed using a JEOL SEM JSM 5800 scanning electron microscope (SEM). The investigation of the suspensions in-

cluded a determination of the density and viscosity measured with an Ostwald viscometer. The densities of the suspensions were calculated as the ratio between the suspension mass and the volume determined with a graduated cylinder at 293 K. Viscosity measurements were conducted at the constant temperature of 293 K. The method involved a determination of the time needed for the distilled water meniscus to pass through the marked spots above and below the reservoir of the Ostwald viscometer. The procedure was repeated 10 times. Afterwards, the same procedure was applied to the suspensions. Dynamic viscosity was determined using the following equation, already presented in the previous research of the authors:[15]

$$\eta_s = \eta_w \frac{t_s \rho_s}{t_s \rho_w} \qquad (1)$$

where η is the dynamic viscosity (Pa s), t presents the value of the measured time (s) and ρ is the specific gravity (g/cm^3). Subscripts s and w represent the suspension and the water, respectively.

To identify the optimum process parameters for an alumina-foam preparation, the effects of the suspension amounts, clay addition and sintering temperature were investigated. Representative high- and low-temperature sintering ceramics were selected according to the available scientific literature and previous researches. The starting α-Al$_2$O$_3$ powder was obtained with a calcination of Al(OH)$_3$ at 1373 K for 3 h. The refractory clay was obtained from Kopovi Ub JSC, Serbia. The α-Al$_2$O$_3$ powder and α-Al$_2$O$_3$–25 clay (mass fractions, w/%) powder mixture were wet-ball milled for 40 h and 8 h, respectively. The refractory clay consisted of 35 % Al$_2$O$_3$, 60 % SiO$_2$, 3 % Na$_2$O + K$_2$O and 2 % CaO + MgO + Fe$_2$O$_3$. The suspensions consisted of α-Al$_2$O$_3$ with w = 1 % sodium carboxymethyl cellulose in water (henceforth referred to as ASCC) and α-Al$_2$O$_3$–25 clay (w/%) (henceforth referred to as A-C), with 35 % and 25 % water amounts, respectively. According to the flow sheet of the technological process of the alumina-foam preparation, presented in the previous research,[15] the polyester foam with 10 PPI was cut into cylinders and soaked in the suspensions for 3 min with constant stirring. Excess suspension was removed using gravity and shaking. The green bodies were dried for 24 h at room temperature. Sintering was conducted at (1573, 1623, 1673, 1723 and 1773) K for 60 min.

The quantity of the applied material after the soaking and drying for 24 h at room temperature was determined from the mass difference between the polymer templates and the green samples, taking into account their volumes. The pore volumes of the green and sintered bodies were examined with an image analysis using the linear intercept method. Series of 10 parallel lines were superimposed on the photographs of the foams and the porosity was determined from the ratio between the total

intercept length of the lines with pores and the total line length, using the following equation:[15]

$$P = \frac{L_p}{L_l} \cdot 100 \ (\%) \qquad (2)$$

where P is the porosity (%), L_p is the total pore-intercept length and L_l is the total line length. The pore diameters and strut thicknesses of the polymer foams and green samples were determined from the pore- and strut-intercept lengths. Measures were conducted taking into account only the pores and struts visible on the top surface of a sample.

The pore volumes of the sintered foams were calculated using the following equation[15]:

$$P_s = \frac{\rho_r - \rho_b}{\rho_r} \cdot 100 \ (\%) \qquad (3)$$

where the real and bulk densities are ρ_r and ρ_b, respectively.

The linear shrinkage after the sintering was calculated using an equation applied in the previous research:[15]

$$S = \frac{L_g - L_s}{L_g} \cdot 100 \qquad (4)$$

where S is the linear shrinkage degree (%), L_g is the mean height of a green body (mm) and L_s is the mean height of the sintered foam (mm).

Uniaxial compression tests of the sintered foams were determined using a hydraulic testing machine INSTRON 1332 - retrofitted Fast track 8800 with 60543 static load cell (± 5 kN capacity), at a piston speed of 0.5 mm min^{-1}. The cylinder-shaped samples were set under a compression plate and the compressive strength was determined from the maximum load at failure and the cylinder base area. The procedure was repeated 3 times for each series of the samples. The microstructures of the sintered foams were analysed with SEM. The microstructure development represents a correlation between the technology and properties.

3 RESULTS AND DISCUSSION

The SEM analysis of the starting powders indicates a presence of the particle sizes below 30 μm and an irregular particle shape with a rough surface morphology in the α-Al$_2$O$_3$ sample (**Figure 1a**). In addition, the presence of clay as the binder, large surface area and energy and the effects of the attractive forces between fine particles resulted in an agglomeration in the α-Al$_2$O$_3$-clay sample (**Figure 1b**). A presence of individual particle sizes of less than 25 μm was noted.

The addition, clay as the binder significantly altered the rheological properties of the suspensions (**Table 1**). The A-C suspension had a higher density in combination with a lower viscosity and was more suitable for applying to a polymer template. The first soaking of the poly-
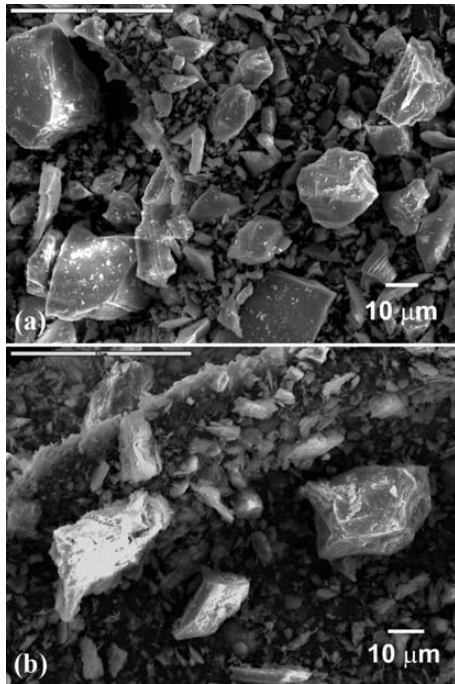
Figure 1: SEM images of starting powders: a) α-Al$_2$O$_3$ powder, b) α-Al$_2$O$_3$-clay powder mixture
Slika 1: SEM-posnetka izhodnih prahov: a) prah α-Al$_2$O$_3$, b) mešanica prahov α-Al$_2$O$_3$-glina

Table 1: Properties of the α-Al$_2$O$_3$ and α-Al$_2$O$_3$–25 clay (mass fractions, w/%) suspensions
Tabela 1: Lastnosti suspenzij z α-Al$_2$O$_3$ in α-Al$_2$O$_3$–25 gline (masni deleži, w/%)

Suspension type	ASCC	A-C
Density/(kg m^{-3})	1980	2096
Viscosity/(Pa s)	4.92×10^{-2}	2.91×10^{-2}

mer foam into the A-C suspension resulted in a complete coverage of the polymer-foam template. The characterisation of green bodies is shown in **Table 2**. The pore size and strut thickness are D and d, respectively. The samples produced using the A-C suspension had an optimum homogeneity and pore volume (78.42 %).

The pore volume decreases (**Figure 2a**) and the intensity of the linear shrinkage increases (**Figure 2b**) as the sintering temperature increases. As a measure of the system activity, the latter is the result of the formation of and an increase in the contact surface between the particles and their movement towards the interior. In the systems based on the ASCC suspension, the optimum sintering temperature of α-Al$_2$O$_3$ was not reached. With
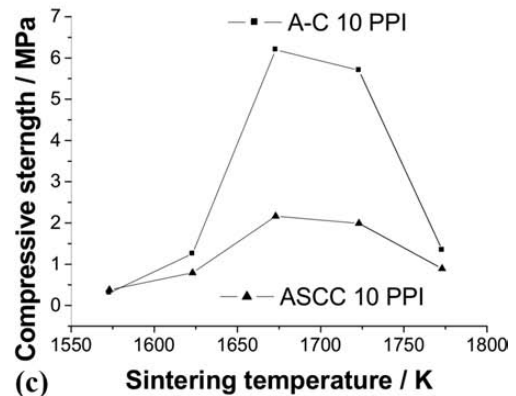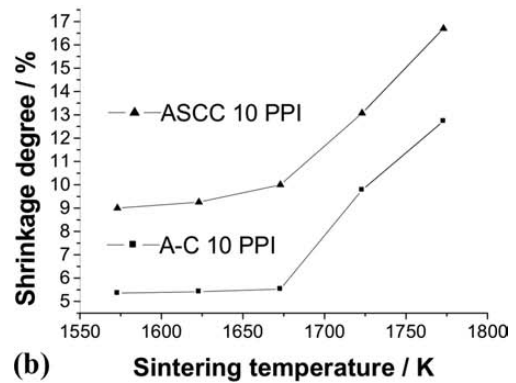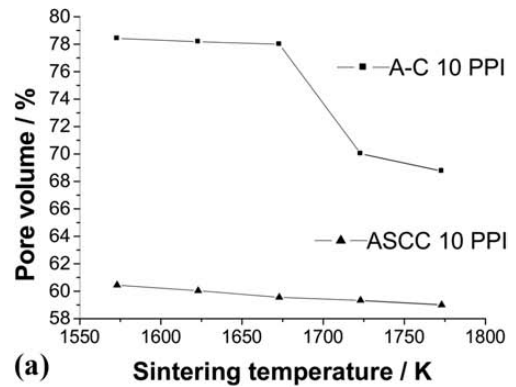

Figure 2: Dependence of: a) pore volume, b) linear shrinkage and c) compressive strength on sintering temperature
Slika 2: Odvisnost: a) volumna por, b) linearnega raztezka in c) tlačne trdnosti od temperature sintranja

the increasing sintering temperature up to 1673 K, the compressive strength increases and then declines rapidly after 1723 K (**Figure 2c** and **Table 3**). It can be concluded that the pore volume and linear shrinkage have an important influence on the values of the compressive strength.

Table 2: Characterisation of green samples
Tabela 2: Karakterizacija zelenih vzorcev

Susp.	Pore vol./%	*Mat. qty. /g cm^{-3}	D_{mean} /mm	D_{max} /mm	D_{min} /mm	Std. errs.	Std. dev.	d_{mean} /mm	d_{max} /mm	d_{min} /mm	Std. errs.	Std. dev.
ASCC	60.45	0.33	2.02	4.10	0.45	0.95	0.14	0.38	0.59	0.20	0.09	0.02
A-C	78.42	0.56	2.30	3.89	0.75	0.79	0.11	0.61	1.30	0.30	0.21	0.03

*Material quantity applied to a polymer foam

The linear shrinkage intensity, as a measure of the system activity, increases with the increasing sintering temperature. A SEM of a strut cross-section of the ASCC-suspension-based foam, sintered at 1573 K, is shown in **Figure 3a**. The gaps that remain in its central part after the polymer combustion are clearly visible. With the increasing sintering temperature, particles of irregular shapes grow from the outer surface of the struts to the interior, reducing the gaps until they are completely eliminated. The above movement of the particles causes a shrinkage of the foam, which is more intense as the sintering temperature increases, until the gaps finally disappear. A SEM of a strut cross-section of the ASCC-suspension-based foam, sintered at 1673 K, is shown in **Figure 3b**; here the gaps were not identified in the center of the struts.
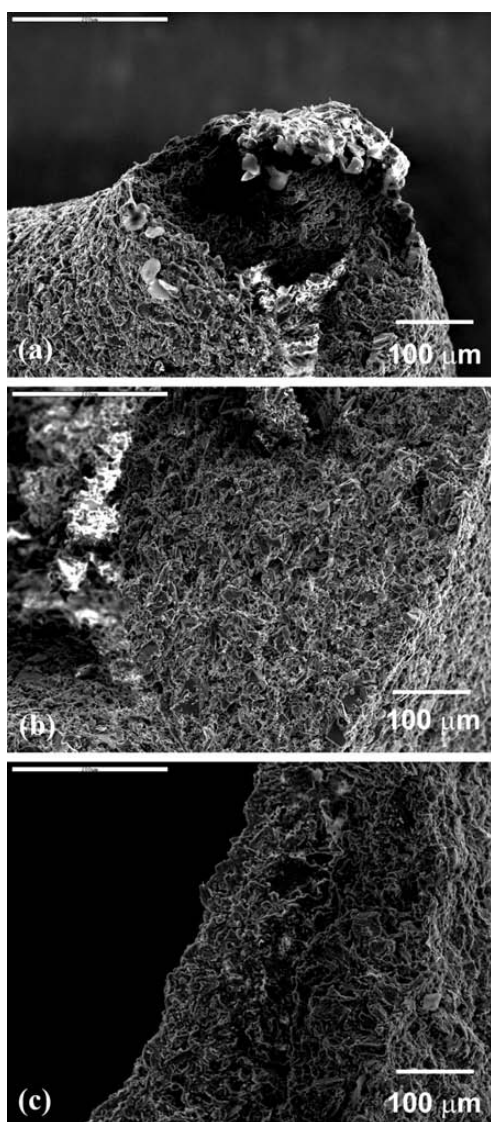

Figure 3: SEM images of a strut cross-section, foam based on ASCC: a) 1573 K, b) 1673 K, c) foam based on A-C, 1573 K
Slika 3: SEM-posnetki prereza opore, pena na osnovi ASCC: a) 1573 K, b) 1673 K, c) pena na osnovi A-C, 1573 K

Table 3: Dependence of the compressive strength on the sintering temperature
Tabela 3: Odvisnost med tlačno trdnostjo in temperaturo sintranja

Material and T/K	Max. load at failure (N)	Mean D/cm	P/MPa	Mean P/MPa	Std. err.	Std. dev.
ASCC – 1573 K	164	2.074	0.4857	0.48	0.0037	0.0064
	168		0.4975			
	166		0.4961			
ASCC – 1623 K	184	2.068	0.5480	0.55	0.0045	0.0079
	189		0.5629			
	185		0.5511			
ASCC – 1673 K	675	2.072	2.0058	2.00	0.0017	0.0030
	674		1.9999			
	676		2.0029			
ASCC – 1723 K	608	2.073	1.8023	1.80	0.0017	0.0029
	607		1.8052			
	609		1.7994			
ASCC – 1773 K	205	2.074	0.6071	0.60	0.0034	0.0059
	201		0.5953			
	203		0.6012			
A-C – 1573 K	167	2.073	0.4950	0.49	0.0017	0.0030
	166		0.4891			
	165		0.4921			
A-C – 1623 K	407	2.071	1.1969	1.20	0.0034	0.0060
	403		1.2029			
	405		1.2088			
A-C – 1673 K	2092	2.072	6.2074	6.20	0.0045	0.0079
	2093		6.2104			
	2097		6.2223			
A-C – 1723 K	1890	2.075	5.5919	5.60	0.0017	0.0030
	1892		5.5978			
	1891		5.5948			
A-C – 1773 K	477	2.075	1.4113	0.49	0.0060	0.0104
	470		1.3906			
	473		1.3994			

In addition, a decrease in the volume porosity occurs. Overall, the increasing shrinking and the reduction in the volume porosity, with the increasing sintering temperature, cause an increase in the compressive strength.

A SEM of a strut cross-section of the foam based on the A-C suspension, sintered at 1573 K, is given in **Figure 3c**. No gaps are identified in its central part. It is evident that at 1573 K the contact formation between individual particles, the growth of the surface contact and the particle movement towards the interior resulted in a removal of the gaps from the central part. This led to a more intense shrinkage, a reduction in the volume porosity and a subsequent increase in the pressure strength, in comparison to the foam based on the ASCC suspensions at the same time-temperature sintering regime.

A SEM of a strut surface in the ASCC-suspension-based foam sintered at 1573 K (**Figure 4a**) clearly indicates a presence of unevenly distributed, irregularly shaped particles and a closer proximity between individual particles, while maintaining their structural inte-
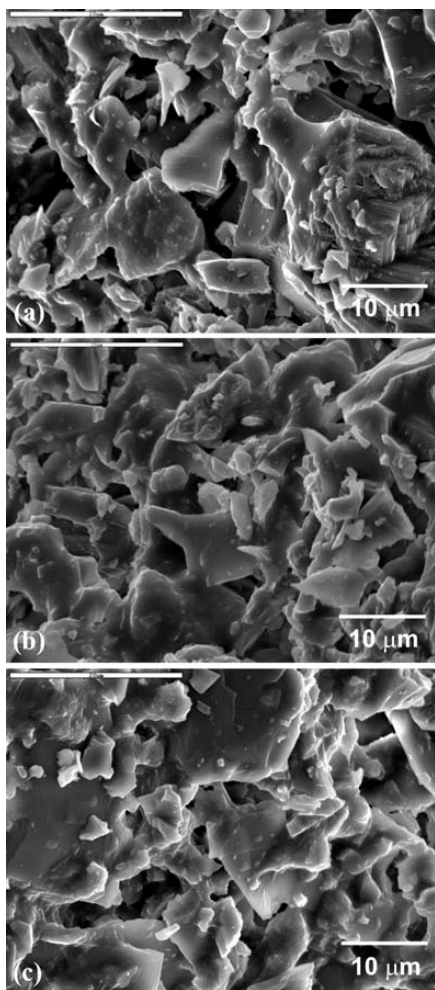
Figure 4: SEM images of a strut surface, foam based on ASCC suspension: a) 1573 K, b) 1673 K, c) 1773 K
Slika 4: SEM-posnetki površine opore, pena na osnovi ASCC-suspenzije: a) 1573 K, b) 1673 K, c) 1773 K

Figure 5: SEM images of a strut surface, foam based on A-C suspension: a) 1573 K, b) 1673 K, c) 1773 K
Slika 5: SEM-posnetki površine opore, pena na osnovi A-C-suspenzije: a) 1573 K, b) 1673 K, c) 1773 K

grity. It is evident that there was no significant increase in the surface contact, which is reflected in the values of the pressure strength. With the sintering temperature increase (**Figure 4b**), the contacts between the particles begin to develop, along with an increase in the contact surface, the latter being only between individual particles. It is noted that the particles lose their structural integrity. The increased surface contact between the particles and the growth of individual particles lead to their rearrangement and improvement of the packaging. A further increase in the sintering temperature (**Figure 4c**) shows a more rapid growth in the contact surface, as well as the individual-particle growth. Large particles grow at the expense of the small ones, found in their surroundings. The particles that appear in the growth direction and are not contiguous with the growing particles do not participate in the process. This microstructure development was causing an intense shrinkage, reducing the pore volume and increasing the compressive strength up to the specific sintering temperature, 1673 K, which was then followed by a decline. The drop in the com-
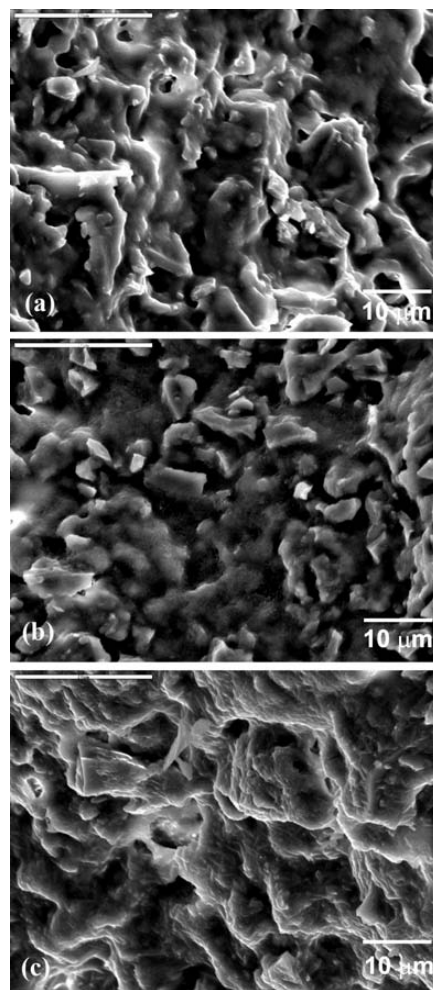
pressive strength, rapid after 1723 K, is the result of a microstructural coarsening and growth of individual particles sintered at 1773 K.

During sintering the samples based on the A-C suspension, there was an intense contact between individual particles at 1573 K (**Figure 5a**) and an increase in the surface contact with a significant reduction in the pore volume (**Figures 5b** and **5c**) at 1673 K and 1773 K. This directly influenced the linear shrinkage degree and increased the compressive strength up to the temperature of 1673 K. The samples sintered at 1723 K achieved approximately the same value of the compressive strength, followed by its significant decrease at the temperature of 1773 K, as a result of an intense microstructure coarsening due to the abnormal growth of individual particles (**Figure 5c**). The best mechanical properties were obtained with the A-C suspension sintered at 1673 K. In comparison to the system based on the ASCC suspension, this system had improved mechanical properties at lower sintering temperatures, owing to the addition of clay as the binder.

In the optimum system, A-C – 10 PPI – 1673 K, a compressive strength of 6.2 MPa was reached. This is higher than for alumina (1.4 MPa and 3 MPa for 5 PPI and 10 PPI, 1.3 MPa for 12 PPI),[4,13] cordierite (2 MPa)[8] and alumina-mullite (1.11 MPa).[7] A higher pore volume (78.42 %) was obtained, compared to porcelain, where the pore volumes were from 26.28 % to 70.59 %.[11] Although the porosity was not sufficiently open, the obtained product is still applicable as a catalyst support. In the present research, the foams with better properties were obtained by sintering at a lower temperature and for a shorter standing time (1673 K for 1h) compared to the foams sintered at 1873 K for 1 h and 5 h.[4,6] The process was shortened compared to the porcelain-foam production, where green bodies were being dried for 72 h at room temperature and additionally for 1 h at 373 K.[11]

4 CONCLUSIONS

The technological process of synthesising the alumina foam as a catalyst carrier was presented. Compared to the current production processes, higher compressive-strength values were achieved at lower sintering temperatures due to an addition of clay as the binder. The technological process was significantly simplified. The best compressive strength of 6.2 MPa was achieved with the system based on the α-Al$_2$O$_3$–25 clay (mass fractions, w/%), polyester foam with 10 PPI, sintered at 1673 K. It has been concluded that the relevant parameters controlling the process are suspension amounts, the clay addition and the sintering temperature. The presented optimisation of these parameters enables a synthesis of monolithic foams with improved mechanical properties with regard to the application and functionality of the catalyst and the quality of the final product with an increased durability and product life.

5 REFERENCES

[1] F. Ribeiro, J. M. Silva, E. Silva, M. Fatima Vaz, F. A. C. Oliveira, Catal. Today, 176 (**2011**), 93–96
[2] P. Ciambelli, V. Palma, E. Palo, Catal. Today, 155 (**2010**), 92–100
[3] A. Donazzi, B. C. Michael, L. D. Schmidt, J. Catal., 260 (**2008**), 270–275
[4] R. Faure, F. Rossignol, T. Chartier, C. Bonhomme, A. Maitre, G. Etchegoyen, P. Del Gallo, D. Gary, J. Eur. Ceram. Soc., 31 (**2011**), 303–312
[5] M. V. Twigg, J. T. Richardson, Ind. Eng. Chem. Res., 46 (**2007**), 4166–4177
[6] F. C. Buciuman, B. Kraushaar-Czarnetzki, Ind. Eng. Chem. Res., 42 (**2003**), 1863–1869
[7] S. Akpinar, I. M. Kusoglu, O. Ertugrul, K. Onel, Ceram. Int., 38 (**2012**), 6163–6169
[8] F. A. Costa Oliveira, S. Dias, M. Fatima Vaz, J. Cruz Fernandes, J. Eur. Ceram. Soc., 26 (**2006**), 179–186
[9] L. Zhang, J. M. F. Ferreira, S. Olhero, L. Courtois, T. Zhang, E. Maire, J. Chr. Rauhe, Acta Mater., 60 (**2012**), 4235–4246
[10] I. Yanase, Y. Yamakawa, H. Kobayashi, J. Ceram. Soc. Jpn., 116 (**2008**), 176–180
[11] M. Al Amin Muhamad Nor, L. C. Hong, Z. Arfin Ahmad, H. Md. Akil, J. Mater. Process. Technol., 207 (**2008**), 235–239
[12] Y. Han, J. Li, Q. Wei, K. Tang, Ceram. Int., 28 (**2002**), 755–759
[13] G. Plesch, M. Vargova, U. F. Vogt, M. Gorbar, K. Jesenak, Mat. Res. Bull., 47 (**2012**), 1680–1686
[14] M. J. Matos, S. Dias, F. A. Costa Oliveira, Adv. Appl. Ceram., 106 (**2007**), 209–215
[15] V. Nikolić, Ž. Kamberović, Z. Anđić, M. Korać, A. Vujović, M. Sokić, Proc. 44th Int. Conf. on Mining and Metallurgy, Bor, RS, 2012; http://www. irmbor.co.rs/index.php/en/, 395–400